Analytic Creeping Wave Model and Measurements for 60 GHz Body Area Networks

Luca Petrillo, Theodoros Mavridis, Julien Sarrazin, David Lautru, Aziz Benlarbi-Delai, Philippe de Doncker

Analytical Creeping Wave Model and Measurements for 60 GHz Body Area Networks

Luca Petrillo*, Theodoros Mavridis*, Julien Sarrazin§, David Lautru¶, Aziz Benlarbi-Delaï§, and Philippe De Doncker *
*Wireless Communication Group, Ecole Polytechnique, Université Libre de Bruxelles
Bruxelles, 1050 Belgium. Email: lpetrill@ulb.ac.be
§Sorbonne Universités, UPMC Univ Paris 06, UR2, L2E, F-75005, Paris, France. Email: julien.sarrazin@upmc.fr
¶Univ Paris Ouest Nanterre La Défense, LEME, F-92410, Ville d'Avray, France. Email: david.lautru@u-paris10.fr

***Abstract*—The propagation of 60 GHz electromagnetic waves around a human body is studied analytically and experimentally. The body is treated here as a circular lossy cylinder, which is an approximation of the human torso. Analytical formulations based on creeping wave theory are given and discussed for both vertical and horizontal polarizations. An exact path gain expression is derived from analytical formulations and a simpler first order approximation is given. Path gain coefficients are shown for frequencies spanning the world available 60 GHz unlicensed band and for several sizes of the torso. Finally, the results of an experimental campaign conducted in an anechoic chamber to isolate the contribution of on-body propagation are reported. The measurement of the distance dependence of the received power on a brass cylinder and on a human body for both vertical and horizontal polarizations confirmed theoretical predictions.**

***Index Terms*—60 GHz propagation; BAN; creeping waves; channel model**

I. Introduction

Miniaturization of integrated components and the more and more pervasiveness of electronic devices let industries and research laboratories imagine Body Area Network (BAN) of wearable computers [1]. One of the most important aspect of future BANs will be the absence of cables connecting worn devices, thus making Wireless BAN (WBAN). Although researches in the past years concentrated mainly on communication systems working around 2.45 GHz [2]–[4] and in the 3.1-10.6 GHz spectrum [5], [6] because of the high availability and low cost of devices, the appearance of the first 60 GHz standards [7] and communicating systems [8] encourages studies in the field of WBAN at this frequency. Indeed, one of the major advantages of 60 GHz communication resides in its limited coverage due to high propagation losses. This involves the possibility of setting up very small wireless networks. Compared to 2.45 GHz, a 60 GHz WBAN would truly permit the coexistence of several personal area networks with many wearable devices communicating around a human body and non-interfering with others WBAN [9].

Link performances between communicating nodes in on-body networks are dependent of their respective positions and body movement and posture. However, an analytical model may be useful to understand experimental data and propagation mechanisms. Furthermore, because of the small wavelength at 60 GHz, full-wave simulations are hardly possible. Hence these computational issues emphasize even more the need for 60 GHz analytical models.

In this work we propose a model based on creeping wave theory to predict the attenuation of vertically and horizontally polarized electromagnetic waves around the human torso at 60 GHz, which extends previous works, conducted on plane surfaces [10], [11]. After recalling creeping waves formulation for the Hertzian dipole radiating above a conducting cylinder, we derive a linear path gain expression permitting to predict the attenuation of vertical or horizontal polarized electromagnetic fields propagating on a circular path around a cylinder having the electromagnetic properties of a human body for frequencies around 60 GHz. Finally, we show measurement results to confirm analytical outcomes.

II. Analytical model

In our study, we consider the interface between air, indicated as medium 0, and a lossy conductor, indicated as medium 1 and representative of the human body, with a complex permittivity $\underline{\varepsilon}_1 = \varepsilon_0\underline{\varepsilon}_r = \varepsilon_0\varepsilon_r - \mathrm{j}\,\sigma/\omega$ and permeability μ_0. Around 60 GHz, the human body can be approximated by only considering the skin, whose electric parameters at these frequencies are $\varepsilon_r = 7.98$ and $\sigma = 36.4$ S/m [12]. In fact, skin depth [13] at 60 GHz is approximately equal to 0.5 mm which is fairly thin if compared to its thickness (2-3 mm). Thus, the 60 GHz model of the human body does not have to take into account the presence of muscles and fat, since the field penetrating the skin is sufficiently attenuated.

We assume a suppressed time dependency $e^{+\mathrm{j}\,\omega t}$, where ω is an angular frequency. Since we are considering on-body communication links, source and observation points will be assumed close to the interface in the air region through the entire communication. The geometry we are taking into account (Fig. 1) is an homogeneous lossy cylinder of radius a, surrounded by air, which is a simplified model for a human torso. In this communication, all the variables are defined in SI units. However, for sake of readability, numerical values are often presented in derivative units.

Both source and observation points will be assumed to lie on a z constant plane, namely $z = 0$, since we are considering a circular path on the cylinder. The distance between source and observation points will be indicated as $\rho_s = \theta a$, where θ is the angle measured between the source and the observation point. Creeping waves formulations will be adopted to calculate vertically and horizontally polarized waves excited by Hertzian dipoles located near the surface of the cylinder.

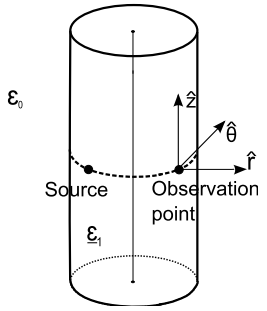

Fig. 1. Geometry of the analytical problem.

III. Hertzian dipole formulation

Dating back to studies concerning electromagnetic wave propagation on the surface of the Earth [14], creeping waves formulations were originally intended to be applied to a Hertzian dipole radiating at the surface of a large (if compared to wavelength) lossy sphere. However, Paknis showed that the same formulations could model the propagation of electromagnetic waves on a circular path around a lossy cylinder [15]. In recent years, such formulations have been adopted to predict the field propagation around human torso and head at 2.45 GHz for on-body communications [16], [17].

A twofold hypothesis permits to use this model: (i), the radius of the cylinder must be larger than free space wavelength and (ii), the complex permittivity of the material filling the cylinder must be much larger than unity. Both conditions are fulfilled in our analysis. Moreover, if the Hertzian dipole and the observation point are not placed on the surface of the cylinder but are in its vicinity at heights h_s and h_r respectively, "height-gain" functions $F(h)$ can be introduced under the hypothesis that both h_s and h_r are smaller than the range ρ_s [18].

We aim to provide a uniform notation for the field radiated by a Hertzian dipole oriented normally or tangentially to the surface of the cylinder and located in its closeness. In the first case, the Hertzian dipole is oriented along the $\hat{r}$ direction. The electric field close to the surface of the cylinder has a r component and a negligible θ component, while the magnetic field is directed towards $\hat{z}$. The electric field is then vertically polarized with respect to the surface of the cylinder and noted E_v corresponding to the r-component. For the second case, the Hertzian dipole is placed parallel to the $\hat{z}$ direction. The case of a Hertzian dipole placed parallel to the $\hat{z}$ axis on the surface of the cylinder is much more complicated than the previous one, since all of the six components of the electromagnetic fields are involved [19]. However, for the scope of this communication we are only interested in the fields propagating around the cylinder in the plane $z = 0$, which is the direction perpendicular to the axis of the dipole. In this case, only the transverse component of the electric field is involved. The electric field is then horizontally polarized and noted E_h corresponding to the z-component.

Formulations for these two cases have been given separately in [15], [18], and can be rewritten as :

$$E_{v,h} = \frac{\mathrm{j}\,\omega\mu_0 I dl}{2\pi}\frac{e^{-\mathrm{j}\,\omega\rho_s/c}}{\rho_s}e^{-\mathrm{j}\,\pi/4}\sqrt{\pi\xi}\cdot \cdot\sum_{i=1}^{\infty}\frac{F_{v,h}(h_s)F_{v,h}(h_r)}{\tau_i^{v,h}-q_{v,h}^2}\exp(-\mathrm{j}\,\xi\tau_i^{v,h}) \tag{1}$$

with

$$F_{v,h} \simeq \frac{W\left(\tau_i^{v,h} - \sqrt[3]{\frac{2}{k_0 a}}k_0 h\right)}{W(\tau_i^{v,h})} \tag{2}$$

$$\xi = \sqrt[3]{\frac{\omega a}{2c}}\frac{\rho_s}{a} \tag{3}$$

$$q_v = -\mathrm{j}\sqrt[3]{\frac{\omega a}{2c}}\sqrt{\frac{1}{\underline{\varepsilon}_r}} \qquad q_h = -\mathrm{j}\sqrt[3]{\frac{\omega a}{2c}}\sqrt{\underline{\varepsilon}_r} \tag{4}$$

and $\tau_i^{v,h}$ are the zeros of

$$W'(\tau_i^{v,h}) - q_{v,h}W(\tau_i^{v,h}) = 0 \qquad i = 1, 2, ... \tag{5}$$

I is the current flowing in the dipole, dl is its length and c is the speed of light in vacuum. $W(\tau)$ is a Fock-type Airy function defined in [14], [15] by $W(\tau) = \sqrt{\pi}\,[B_i(\tau) - \mathrm{j}\,A_i(\tau)]$. F is the "height-gain" function.

IV. Path Gain

In order to give a practical, ready to use approximation of the decay of the electric field on a circular cylinder having the electromagnetic properties of the human body around 60 GHz, two zones with respect to ρ_s are defined. The first one, $0 < \rho_s < \rho_s^T$, is the zone where the fields radiated by a Hertzian dipole located close to the surface of the cylinder cannot be approximated by only the first term of (1). Therefore, more than one zero of (5) need to be taken into account. In this zone, precise evaluation of the fields decay is strongly dependent on the height of the Hertzian dipole above the surface of the cylinder, mainly because the field reflected off the cylinder surface can add constructively or destructively to the direct field. Consequently, considering also that this zone is restricted to small tangential distances from the source, we will not give an expression of the path gain in this zone.

In the second zone, $\rho_s > \rho_s^T$, only one zero of (5) is needed to compute (1). Here, the field exponentially decays and it is commonly known as creeping wave.

In [19], ρ_s^T is some value much greater than $a\sqrt[3]{\frac{2c}{\omega a}}$ for source and observation points close to the interface between the air and the conductor. This condition can be relaxed and a heuristic expression for the choice of ρ_s^T can be given by introducing the relative error in linear scale between equation (1) calculated with the first 10 terms of the sum, and equation (1) calculated with only the first term of the sum. We found that $\rho_s^T = 0.2a + 0.04$ permits to keep this error smaller than 5% for values of h_s and h_r smaller than 5 mm, for frequencies comprised between 57 and 66 GHz, and BAN scenarios (0.1 m$\leq a \leq$0.2 m).

In order to give a path gain expression of E_v in the second zone, we have to note that for the first term in (1), the ρ_s dependency of the module of E_v is:

$$|E_v(\rho_s)| = E_0 e^{\mathrm{Im}[\tau_1^v]\xi}/\sqrt{\rho_s} = E_0 e^{-m_v\rho_s}/\sqrt{\rho_s} \tag{6}$$

$$m_v = -\,\mathrm{Im}[\tau_1^v]\sqrt[3]{\frac{\omega a}{2c}}\frac{1}{a} \tag{7}$$

where $\mathrm{Im}[\tau_1^v]$ is the imaginary part of τ_1^v. Therefore, with respect to a reference distance $\rho_{s0} \geq \rho_s^T$, the path gain is:

$$G(\rho_s) = G(\rho_{s0}) - 10\log_{10}\frac{\rho_s}{\rho_{s0}} - n_v(\rho_s - \rho_{s0}) \tag{8}$$

$$n_v = 20 m_v \log_{10} \mathrm{e} \tag{9}$$

In the above expressions, G is the path gain expressed in dB and n_v is the power decay exponent for vertical polarization. It is worth noting that (8), with n_v computed using (9), is exactly equivalent to E_v evaluated with only the first zero of (5). However, an approximate expression of (8) starting from a first order series expansion of the logarithm can be derived. Then, expanding around ρ_{s0} :

$$G(\rho_s) \simeq G(\rho_{s0}) - n'_v(\rho_s - \rho_{s0}) \tag{10}$$

with

$$n'_v = n_v + \frac{10}{\rho_{s0} \ln 10} \tag{11}$$

The error incurred in approximating (8) by (10) is equal to the residual of the Taylor series of the logarithm, which is equal to $10(\rho_s - \rho_{s0})^2/(2\rho_{s0}^2 \ln 10)$.

The same reasoning can be carried out for the path gain of horizontally polarized waves. Thus, we can define two new power decay exponents n_h and n'_h, which are:

$$n_h = -20 \,\mathrm{Im}[\tau_1^h] \sqrt[3]{\frac{\omega a}{2c}} \frac{1}{a} \log_{10} \mathrm{e} \tag{12}$$

$$n'_h = n_h + \frac{10}{\rho_{s0} \ln 10} \tag{13}$$

TABLE I
PATH GAIN SLOPE FOR VERTICAL AND HORIZONTAL POLARIZATION, FOR DIFFERENT FREQUENCIES AND VALUES OF a (n_v *and* n_h *are expressed in dB/cm,* σ *is expressed in S/m.)*

	a=0.10 m	$a = 0.15$ m	$a = 0.20$ m
57 GHz			
$\varepsilon_r = 8.34$	n_v=4.10	n_v=3.29	n_v=2.82
$\sigma = 35.9$	n_h=6.67	n_h=5.11	n_h=4.23
60 GHz			
ε_r=7.98	n_v=4.23	n_v=3.40	n_v=2.91
σ =36.4	n_h=6.78	n_h=5.20	n_h=4.30
63 GHz			
ε_r=7.65	n_v=4.35	n_v=3.50	n_v=3.00
σ =36.8	n_h=6.89	n_h=5.28	n_h=4.37
66 GHz			
ε_r=7.37	n_v=4.48	n_v=3.6	n_v=3.09
σ =37.2	n_h=7.00	n_h=5.36	n_h=4.44

Path gain results are shown in Table I: different values of the radius of the cylinder have been chosen and frequencies covering the world-wide available spectrum around 60 GHz are shown as well. n'_v and n'_h can be calculated from the reported values of n_v and n_h by using equations (11) and (13) and by choosing a value of ρ_{s0} greater than ρ_s^T.

It is interesting to compare 60 GHz creeping wave attenuation with similar results obtained at 2.45 GHz [16], [17]. For vertical polarization, at 60 GHz the fields attenuate at the rate of nearly 3 dB/cm, while at 2.45 GHz the attenuation rate is only 0.73 dB/cm for a radius equal to 20 cm. Consequently, Table I represents useful insights for the power management and routing strategies of a 60 GHz BAN.

V. MEASUREMENTS

An experimental campaign was carried out in an anechoic chamber to measure the propagation at the surface of a cylindrical body. All measures are performed with an Agilent E8361C Vector Network Analyzer in an anechoic chamber. Since large losses due to the coaxial cables were found at 60 GHz (6 dB/m), the VNA was placed inside the anechoic chamber to limit the length of the cables feeding the field probes. The measured parameter was $|S_{21}|^2$ between the probes.

A. PEC measurements

In a first step we compared the creeping wave model at 60 GHz with the field measured on a brass cylinder of radius equal to 20 cm and of height equal to 1 m. Brass offers a good trade-off between mechanical properties, price and high electric conductivity, which allows to assimilate it to PEC for the frequency under exam (brass conductivity is equal to 2.56×10^7 S/m [20]). The brass cylinder was vertically mounted on a rotor and could rotate around its axis. A pyramidal horn antenna has been used as transmitter. It has a gain of 20 dB and a beamwidth of 10°. The aperture size is 2.3 cm x 3 cm. It has been mounted directly on the surface of the cylinder, at middle height. A field probe has been realized by fixing a second identical antenna on a vertical stand. The probe was then moved at the surface of the cylinder, at the same height as the source. Different distances between source and probe were achieved by rotating the cylinder (only the transmitter is fixed to the cylinder). Both antennas are located tangentially to the surface of the cylinder and the distance between the horns and the cylinder was equal to zero. Consequentially, the distance between the phase center of the horns and the cylinder was equal to half the horns' aperture: 1.5 cm for vertical polarization and 1.15 cm for horizontal polarization. A schematic representation of the measurement setup is drawn in Fig. 2. The VNA noise level is equal to approximately -100 dB.

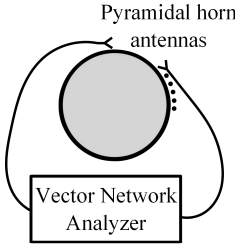

Fig. 2. Measurement setup. Black dots indicate different measurement points.

In Fig. 3 we have reported the results of the measurement on the brass cylinder for both polarizations. By comparison with the predicted results obtained with (8) normalized with respect to the first measurement, it can be concluded that the field in the zone we have measured decays as a creeping wave on the

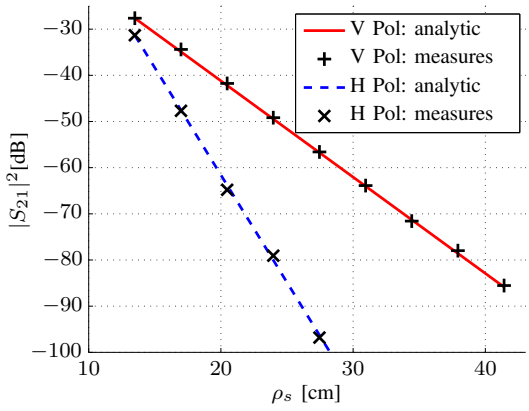

Fig. 3. Vertical and horizontal polarization measurement results compared with analytical attenuation prediction for a PEC cylinder of radius a=0.2 m.

surface of the cylinder. Since a horn antenna can be considered as a composition of dipoles of different heights exciting fields with the same attenuation, it is possible to compare the attenuation rate of horn antennas and dipoles [11]. Linear regressions of the plotted data exactly correspond to analytical results. For vertical polarization the decay coefficient is equal to 2.08 dB/cm, while for horizontal polarization we found 4.65 dB/cm.

B. Body measurements

Fig. 4. Antennas setup for body measurement.

A second measurement set up was carried out in order to measure the field propagating around human torso. The aim of these measurements is to demonstrate that creeping wave formulations can be used to predict the attenuation of the field propagating at the surface of the torso in a circular path. The arms were raised during measurement (see Fig. 4), thereafter they do not influence the measurement. A belt made of cotton (thickness: 5 mm) was used to fix the antennas to the torso and has virtually no influence on the measurements [21]. However, two main difficulties were expected. Firstly, we were of the opinion that if source and receiving probes were on the same side of the torso, then a flat propagation surface would have led to a different propagation mechanism, better described by Norton's formulations [22]. Secondly, we were aware that the fast decay of the creeping wave would have limited the maximum distance from source and probe, for which measurements can be possibly conducted taking into account the VNA noise floor. Consequently, we chose to measure the decay of the field radiated by a horn antenna placed on the front side of the torso, approximately on the nipple, in the curved region of the torso itself, under the arm. For this measurement, the VNA noise level was approximately equal to -75 dB, which is higher than PEC measurement since averaging was limited due to the need of faster acquisitions. In Table II we have summarized the relevant parameters of these measurements.

TABLE II
RELEVANT GEOMETRICAL PARAMETERS FOR HUMAN TORSO MEASUREMENTS

Parameter	Symbol	Value
Torso perimeter		0.9 m
Approximated radius	a	15 cm
Height of the subject		1.68 m
Gender		Male
Tangential distance step	$\Delta\rho_s$	1.5 cm
Number of steps		9
Source position		Left nipple
Radial start value		19 cm

Measurements are plotted in Fig. 5 and 6. In the same figure we plotted the analytical prediction using creeping wave formulas for a cylinder of radius equal to 15 cm having the same electromagnetic properties of human skin at 60 GHz. Linear regression curves are plotted as well. For vertical polarization, the decay coefficient is equal to 3.18 dB/cm, while for horizontal polarization it is equal to 4.48 dB/cm. Deviation from linearity in both measurements for large ρ_s is due to reaching of noise floor. Although dispersion around the theoretical result is higher than in the PEC case, Figs. 5 and 6 show that the path loss profile of the field radiated by an electromagnetic source at the surface of the torso can be modeled in the curved zone by assuming that the torso has a circular section of radius equal to its perimeter divided by 2π.

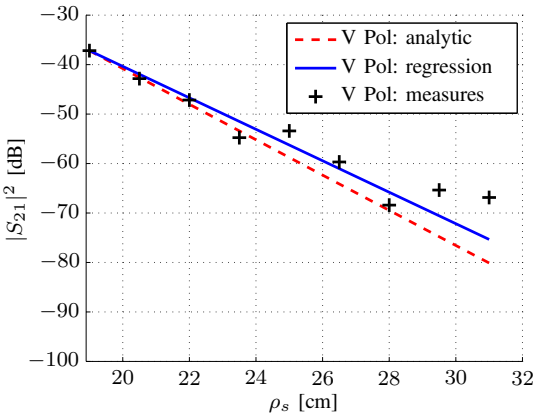

Fig. 5. Vertical polarization measurement results compared with the theoretical attenuation prediction on a human torso of radius a=0.15 m.

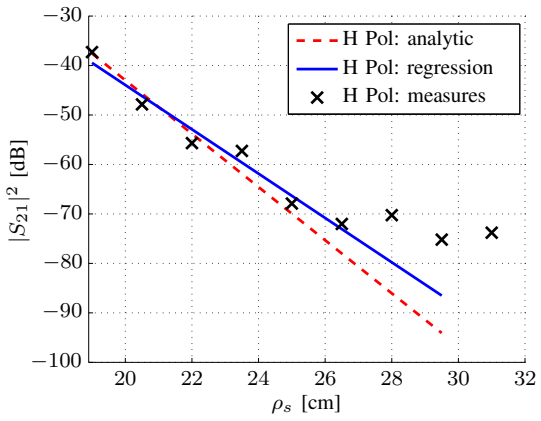

Fig. 6. Horizontal polarization measurement results compared with the theoretical attenuation prediction on a human torso of radius a=0.15 m.

VI. Conclusion

In this paper creeping wave formulation for both vertical and horizontal polarized electromagnetic waves traveling on a circular path around a cylinder are given. A linear path gain has been derived and values of the approximated power decay exponent have been summarized for different frequencies and values of the radius of the cylinder. Measurements on the torso of a real human body at 60 GHz show that the path loss of the field radiated by an electromagnetic source at the surface of the torso can be modeled in the curved zone by assuming that the torso has a circular section of radius equal to its perimeter divided by 2π.

Acknowledgment

The authors would like to thank Mr Y. Chatelon for cylinder manufacturing and Prof. B. Huyart, Mr A. Khy and Dr. R. Mohellebi from Telecom ParisTech for their helpful advice and willingness.

References

[1] P. S. Hall and Y. Hao, *Antennas and Propagation for Body-Centric Wireless Networks*. Artech House Publisher, 2006.

[2] I. Khan et al., "Diversity performance analysis for on-body communication channels at 2.45 GHz" *Antennas and Propagation, IEEE Transactions on*, vol. 57, pp. 956-963, 2009.

[3] R. DErrico and L. Ouvry, "A statistical model for on-body dynamic channels", *International Journal of Wireless Information Networks*, vol. 17, pp. 92-104, 2010.

[4] L. Liu et al., "An analytical modeling of polarized time-variant on-body propagation channels with dynamic body scattering", *EURASIP Journal on Wireless Communications and Networking*, vol. 2011, 2011.

[5] S. Van Roy et al., "A Comprehensive Channel Model for UWB Multisensor Multiantenna Body Area Networks", *Antennas and Propagation, IEEE Transactions on*, vol. 58, pp. 163-170, 2010.

[6] A. Alomainy et al., "Transient Characteristics of Wearable Antennas and Radio Propagation Channels for Ultrawideband Body-Centric Wireless Communications", *Antennas and Propagation, IEEE Transactions on*, vol. 57, pp. 875-884, 2009.

[7] T. Baykas et al., "IEEE 802.15.3c: the first IEEE wireless standard for data rates over 1 Gb/s", *EURASIP Journal on Wireless Communications and Networking*, vol. 9, pp. 114-121, 2007.

[8] Vizio, Inc. Universal Wireless HD Video and Audio Kit (XWH200), http://www.vizio.com/accessories/xwh200.html.

[9] Y. Nechayev et al., "Use of motion capture for path gain modelling of millimetre-wave on-body communication links", *Antennas and Propagation (ISAP), 2012 International Symposium on IEEE*, Nanjing, RC, 2012, pp. 987-990.

[10] M. Grimm and D. Manteuffel, "Evaluation of the Norton Equations for the Development of Body-Centric Propagation Models", *Proc. 2012 EUCAP*, Prague, CZ, 2012, pp. 311-315.

[11] N. Chahat et al., "On-body Propagation at 60 GHz", *Antennas and Propagation, IEEE Transactions on*, vol. 61, pp. 1876-1888, 2013.

[12] P. A. Hasgall et al., "ITIS Database for Thermal and Electromagnetic Parameters of Biological Tissues", Version 2.2, July 11th, 2012, www.itis.ethz.ch/database.

[13] E. C. Jordan and K. G. Balmain, *Electromagnetic Waves and Radiating Systems, 2nd edition*. Chs 5, Prencite-Hall, Inc., Englewood Cliffs, 1968.

[14] V. Fock, "Diffraction of Radio Waves around the Earth's Surface", *Acad. Sci. USSR. J. Phys.*, vol. 9, pp. 255-266, 1945.

[15] R. Paknis and N. Wang, "High-Frequency Surface Field Excited by a Magnetic Line Source on an Impedance Cylinder", *Antennas and Propagation, IEEE Transaction on*, vol. 35, pp. 293-298, 1987.

[16] G. A. Conway et al., "An Analytical Path-Loss Model for On-Body Radio Propagation", *Electromagnetic Theory (EMTS), 2010 URSI International Symposium on*, pp. 332-335, 2010.

[17] T. Alves, B. Poussot and J. M. Laheurte, "Analytical Propagation Modeling of BAN Channels Based on the Creeping-Wave Theory", *IEEE Trans. Antennas Propag.*, vol. 59, pp. 1269-1274, 2011.

[18] K. Li and Y. L. Lu, "Electromagnetic Field from a Horizontal Electric Dipole in the Spherical Electrically Earth Coated with N-Layered Dielectrics", *Progress in Electromagnetic Research, PIER*, **54**, pp. 221-244, 2005.

[19] R. W. P. King, G. J. Fikioris and R. B. Mack, *Cylindrical Antennas and Arrays*. Chs 8 and 9, Cambridge University Press, Cambridge, 2002.

[20] C. A. Balanis, *Advanced engineering electromagnetics*, Wiley, New York, 1989.

[21] A. R. Guraliuc et al., "Effect of Textile on the Propagation Along the Body at 60 GHz", *Antennas and Propagation, IEEE Transaction on*, 2013.

[22] K. A. Norton, "The Physical Reality of Space and Surface Waves in the Radiation Field of Radio Antennas", *Proceedings of the Institute of Radio Engineers*, **25**, 9, pp. 1192-1202, 1937.